

Key words:

SETI, Computer simulations, Statistics

Abbreviations:

SETI: Search for Extraterrestrial Intelligence,

CCN: causally connected node,

SFC: surface of first contact,

SLC: surface of last contact,

DE: Discrete Event,

GHZ: Galactic Habitable Zone

Author for correspondence:

Lares M, Email: marcelo.lares@unc.edu.ar

Probability of causal contact between interstellar civilizations through MonteCarlo simulations

Lares M.^{1,2}, Funes J. G.^{1,3} & Gramajo L.^{1,2}

¹CONICET, Argentina

²Universidad Nacional de Córdoba, Observatorio Astronómico de Córdoba, Argentina

³Universidad Católica de Córdoba, Argentina

Abstract

The abundance of intelligent civilizations in the galaxy is a longstanding question, which is often conceptualized as the problem of the lack of received communication or the Fermi paradox. Most efforts on the estimation of a number of intelligent civilizations are centered on the Drake equation, although its factors are affected by large uncertainties, and it lacks a temporal nature. A alternative approach uses detailed numerical simulations of the galaxy and recipes for the rates of the formation of stars and planets, and even for the origin of life. Here we present numerical simulations of stochastic processes of emergence of civilizations with communication capabilities, based on minimal assumptions, and analyze the causal connections among them. The analysis of the rate of causal contacts as a function of the mean number of civilizations, the mean lifetime span distribution and the maximum distance a civilization can send signals is presented, and used as a framework to discuss the spatial and temporal structure of a populated galaxy within several different scenarios. Our results indicate that, given the large distances involved, causal contacts between civilizations are very rare. Additionally, the odds to make a contact in a few years of monitoring, assuming a perfect detection rate, are low for most models, with the exception of models which propose a galaxy densely populated with long lived civilizations. The probability of causal contacts increases with the mean lifetime of civilizations much more significantly than with the mean number of active civilizations for a given time window.

1. MOTIVATIONS

The Drake equation (Drake, 1962) offers a very helpful educated guess, a rational set of lenses –the factors in the equation– through which to look at future contacts with a technologically advanced civilization in the Milky Way. The equation quantifies the number of civilizations from whom we might receive an electromagnetic signal. For a comprehensive review and analysis of each term of the equation see Vakoch & Dowd (2015). Prantzos (2013) proposes a unified framework for a joint analysis of the Drake equation and the Fermi paradox concluding that for sufficiently long-lived civilizations, colonization of the Galaxy is the only reasonable option to gain knowledge about other life forms. Haqq-Misra & Kopparapu (2018) discuss the dependence of the Drake equation parameters on the spectral type of the host star and the time since the galaxy formed and examine trajectories for the emergence of communicative civilizations over the history of the galaxy. The abundance of intelligent civilizations in the galaxy is a longstanding question, which is often conceptualized as the problem of the lack of received communication or the Fermi paradox (Barlow, 2013a; Sotos, 2019; Forgan, 2017a).

There are many proposals aimed at solving this paradox, which make use of statistical (Solomonides et al., 2016; VanHouten, 2018; Horvat, 2006; Maccone, 2015) or stochastic approaches (Forgan, 2009; Bloetscher, 2019; Glade et al., 2012; Forgan & Rice, 2010), analytical interpretations of the Drake equation (Prantzos, 2013; Smith, 2009) or more speculative proposals (Barlow, 2013b; Lampton, 2013; Conway Morris, 2018; Forgan, 2017b). However, the uncertainties in the factors of the Drake equation make it less prone to a formal application in order to define searching strategies or to compute the actual number of extraterrestrial intelligences, but is a key tool to organize the discussion around the problem of their abundance in the Galaxy (Hinkel et al., 2019), which is noticeable dominated by the fact that despite decades of effort not a single extraterrestrial intelligence, if any, has been detected so far. Some modifications to the original idea of the equation have tried to imprint a stochastic nature, or to propose a probabilistic approach, or to consider the temporal structure which is missing in the equation.

Temporal aspects of the distribution of communicating civilizations and their contacts have also been explored by several authors (Fogg, 1987; Forgan, 2011; Balbi, 2018; Balb, 2018; Horvat et al., 2011), as well as efforts on considering the stochastic nature of the Drake equation (Glade et al., 2012). The simulation approach has also been considered (Forgan et al., 2016; Vukotić et al., 2016; Murante et al., 2015; Forgan, 2009, 2017b), although with a similar problem that consists on the large number of parameters which are either unknown or largely uncertain. In this work, we propose to avoid the frequentist approach of the Drake equation and to explore a parameter space, where instead of computing a final number, we provide a statistical distribution that gives conditional probabilities. This is an exploratory analysis that aims at providing a numerical tool to discuss not the several theoretical problems summarized by the Drake equation factors, but the different scenarios on the basis of statistical heuristics. The approach proposed here should be considered as a compromise between the uncertainties of the frequentist approach and the detailed recipes required on the simulation approach. We then provide a numerical framework to explore via simulations a parameter space of unknown observables in order to discuss different scenarios and their consequences in terms of the probability of making contacts. The only fact that can be stated with certainty is that for the number of years SETI projects have been working we have not received any signal, at least within the technical possibilities and the conditions established by SETI (Tarter, 2001). This arguably astonishing result has led to the Fermi paradox, which states an apparent contradiction between the high estimation of the abundance of life in the Galaxy and the lack of their detection (VanHouten, 2018). The lack of detection has also inspired to a number of alternative proposals for new SETI strategies (Forgan, 2019; Balbi, 2018; Loeb & Zaldarriaga, 2007; Maccone, 2010; Tarter et al., 2009; Enriquez et al., 2017; Loeb et al., 2016; MacCone, 2011; Lingam & Loeb, 2018; Wright et al., 2015; MacCone, 2013; Maccone, 2014b; Harp et al., 2018; Forgan, 2013, 2017b; Funes et al., 2019).

The discrete events method for simulating a stochastic process is an approximation that allows to study the behaviour of complex systems, by considering a sequence of well defined discrete events. The simulation is carried out by following all the variables that describe the system, that constitute the state of the system. The evolution of the process, then, is described as a set of changes in the state of the system. In this context, an event produces a specific change in the state, that can be triggered by random variables that encode the stochastic nature of the physical phenomenon. The process involves following the changes on the state of the system, defining the initial and final states, defining a method that allows to keep track of time progress, and maintaining a list of relevant events. (REESCRIBIR!!)

In a recent work, (Balbi, 2018) use a statistical model to analyze the occurrence of causal contacts between civilizations in the Galaxy. The author highlights the effect of evolutionary processes when attempting to estimate the number of communicating civilizations that might be in causal contact with an observer located on the Earth. Čirković (2004) also emphasize the lack of temporal structure in the Drake equation.

Bloetscher (2019) uses a probabilistic approach, though still strongly motivated by the Drake equation, to obtain a probabilistic measure for the number of civilizations in the Galaxy. To that end, perform MonteCarlo Markov Chains over each factor

of the Drake equation, and combine the means to obtain a probabilistic result. It is worth mentioning that the author proposes a log-normal target distribution to compute the posterior probabilities. This approach, which assigns probability distributions to the Drake factors. This study concludes that there is a very low probability for Earth to make contact with another extraterrestrial civilization. Smith (2009) uses a analytical model to compute the probabilities of contact between two randomly located civilizations, and the waiting time for the first contact, assuming a fixed maximum broadcasting distance. Balbi (2018) investigate the chance of communicating civilizations making causal contact within a volume surrounding the location of the Earth, using a statistical model to compute the occurrence of causal contacts. The author stresses the fact that the causal contact requirement involves the distance between civilizations, their lifespan and their times of appearance. This is important since the time it takes the light to travel across the Galaxy is much lesser than the lifetime of the Galaxy. Balbi (2018) fix the total number of civilizations and explore the parameter space that comprise three parameters, namely, the distance to the Earth, the time of appearance and the lifespan of the communicating civilization. Each of these three variables are drawn from a random distribution. The distribution of the distances results from a uniform distribution of civilization within the plane of the Galaxy. For the distribution of the characteristic time of appearance, the author explores and exponential and a truncated Gaussian distributions. For the distribution of the lifespans, the author chooses an exponential distribution. The radius of influence is set to 1000 ly. Balbi (2018) finds that the fraction of communicating civilizations vary with the choice of the statistical distribution for the time of appearance. For all analyzed distributions, the fraction corresponding to a mean lifetime of 10^9 years and for a maximum radius for the detection of the signal of 1000 yr, is roughly 0.1. Vukotić & Čirković (2012) propose a simulation approach based on probabilistic cellular automata (PCA) modeling. In this framework, a complex system is modeled by a lattice of cells which evolve at discrete time steps, according to transition rules that take into account for each cell the states of its neighbour cells. The authors implement a PCA model to a network of cells which represent life complexity on a 2-dimensional annular ring resembling the GHZ. The authors set the GHZ between a minimum radius of 6 kpc and a maximum radius of 10 kpc. Within this framework, the authors also make several MonteCarlo simulations and analyze ensemble-averaged results. This work aims at analyzing the evolution of life, although it does not account for the network of causal contacts among technological civilizations.

In this work we address the problem of the temporal and spatial structure of the distribution of communicating civilizations, by exploring the hypothesis space over a minimal set of parameters. In Sec. 2. we introduce the methods and discuss the candidate distributions for the statistical aspects of the times involved in the communication process. Then, we present our results in Sec 3., with special emphasis on the statistical distributions of the duration of causal contacts in one or both directions, the possible differences on the position of a civilization on the Galaxy and the distribution of time intervals for the waiting of the first contact, always as a function of the three simulation parameters. Finally, in Sec. 4. we discuss our results and future research directions.

2. METHODS AND WORKING HYPOTHESES

Simulations are suitable tools to analyze systems that evolve with time and involve randomness. An advantage of simulations compared to theoretical approaches, is that the former usually require less assumptions and simplifications, and can be applied to systems where a theoretical model can not be found. In particular, many complex stochastic processes that can be described by the evolution of the state of a system, can be efficiently modeled with the discrete-event (hereafter, DE) simulation approach. A system described with the DE paradigm is characterized by a set of actors and events, where actors interact causally through a series of events on a timeline and process these events in chronological order (Ptolemaeus, 2014; Chung, 2003; Ross, 2012). Each event produces changes in the values of the variables that define the process, and thus the corresponding change in the state of the simulated system. This method is well suited for the particular case of the diffusion of intelligent signals in the Galaxy, and allows to explore several models easily. We simulate the statistical properties of a set of points in space and time that have a causal connection at light speed, hereafter dubbed "causal contact nodes" (CCN). We chose this generic name in order to stress the fact that in this analysis no broadcasting or lookout activities are required, and therefore not actual messages are considered, only the causal contact. For the special case of a fully efficient node that emits and receives isotropically, a causal contact node can be considered as a broadcasting station that has the ability to detect signals through an active lookout program. Also, it is worth mentioning that this is a general approach, and not necessarily a CCN is the host of an intelligent civilization. It can be associated with a planet where life has developed, became intelligent, reached the skills required to find the right communication channel, sustain a search and establish a contact. Alternative message processing entities could be considered, for example interstellar beacons where life has ceased to exist but continue with its emission or communication stations established by probes or left intentionally by intelligent beings (see, e.g., Peters, 2018; Barlow, 2013b). In principle, these strategies could affect our results since it would be easier to configure a cluster of CCNs that spread in time. However, we do not consider this highly speculative alternatives at this point. For the purpose of this analysis, only the communication capability is relevant, since we study the causal contacts between the locations. The system is defined by a number of actors that represent CCNs and appear at different instants in time, generating events that produce meaningful changes in the variables that describe the system, i.e., in the arrangement of CCNs and their network of causal contacts. For example, the appearance of a new CCN in a region which is filled with a signal emitted by another CCN, will increase the number of active CCNs and the number of pairs of CCNs in causal contact. Assuming some simple hypotheses, the discrete events method can be performed taking into account a small number of variables, which allow to analyze the variation of the results in the model parameter space.

In what follows, we describe the experimental setup chosen to estimate the probabilities of causal contacts and several derived quantities in terms of three independent parameters, namely, the mean time span between the appearance of consecutive CCNs, $\langle\tau_a\rangle$, their mean lifetime $\langle\tau_s\rangle$, and the maximum distance a signal can be detected by another CCN (D_{max}). Intuitively, the shorter

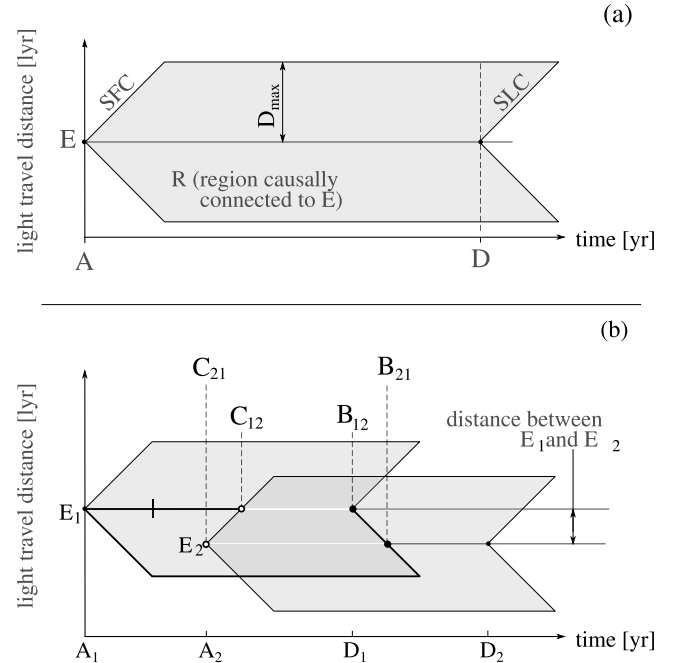


Fig. 1. Space-time diagrams showing a schematic representation of the different stages in the development of causal contact node (CCN). Panel (a) represents the region R in space and time which is causally connected to the emitter (left vertex), following an "A" type event ("Awakening") in which the node acquires the communication capability. The sphere of first contact (SFC) is a sphere centered on the emitter that grows until its radius reaches the D_{max} distance, in which the power of a signal would equal the detectability threshold. In the Figure this sphere is represented by the left triangle of the region R . The surface of last contact (SLC) is another sphere that grows from a "D" event ("Doomsday"). The region which is causally connected to the emitter is then limited by these two spheres, and has the shape of a sphere or of a spherical shell, depending on the time. The temporal intervals for the communication between two CCNs are represented in the panel (b). The receiver CCN E_1 can listen signals from the emitter CCN E_2 , from the "Contact" event ($t=C_{12}$) up to the "Blackout" event ($t=B_{12}$). Similarly, the receiver CCN E_2 can listen signals from the emitter CCN E_1 , from $t=C_{21}$ up to $t=B_{21}$.

the τ_a parameter and the larger the τ_s and D_{max} parameters are, the greater the probability of the existence of causal contacts between pairs of CCNs would be. We also need to propose theoretical distribution functions for both the distribution of lifespans (τ_s) and the distribution of the number of CCNs per unit time (Maccone, 2014a; Sotos, 2019), related to the time span between the appearance of consecutive CCNs (since when $\langle\tau_a\rangle$ is shorter, it produces a greater density of CCNs). The shapes of these distributions are set to a fixed law, as discussed in Sec. 2.1..

We illustrate in the Fig. 1 the schematic representation of the region causally connected to the central CCN. To this end, we use space-time diagrams, where time is represented on the horizontal axis, and space is represented in the vertical axis. In particular, we plot on the vertical axis the distance travelled by a signal at light speed from the emitter. Panel (a) represents the region R (shaded

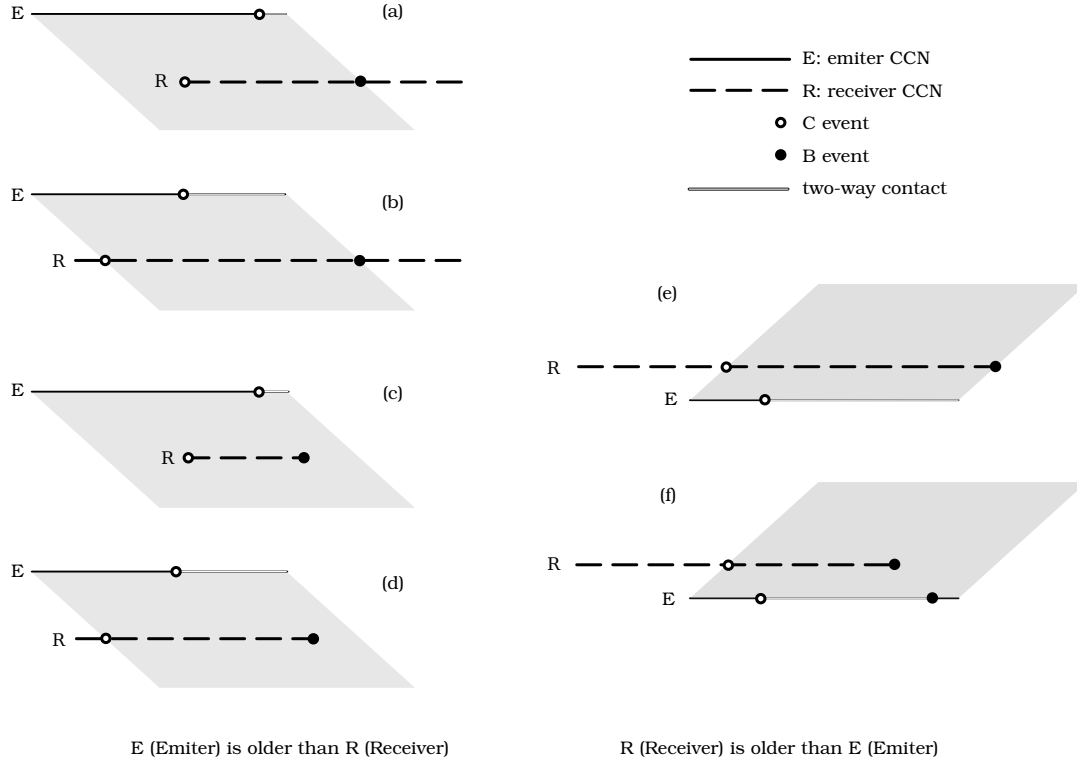


Fig. 2.: Schematic representation on space-time diagrams of the possible cases in which a CCN E (Emitter, solid line) can be in causal contact with a CCN R (Receiver, dashed line). Causal contact can be produced either if the emitter CCN appears before (left) or after (right) the receiver CCN. The causal contact in which the receiver can have access to the signal from the emitter is produced between the C event (Contact, open circles) and the B event (Blackout, filled circles). The duration of the causal contact in one direction depends on several factors, mainly the time lag between the awakening events (horizontal separation in the space-time diagrams) and the distance between the CCNs (vertical separation in the space-time diagrams). The different configurations must be taken into account in order to obtain the list of the upcoming events. The time intervals for a two-way communication to be possible are indicated in double lines.

polygon) in space and time which is causally connected to the emitter (left vertex), following an "A" type event in which the node acquires the communication capability. The sphere of first contact (SFC) is a sphere centered on the emitter, represented in the Figure by the left angle of the region R . This sphere grows until its radius reaches the D_{max} distance, in which it would be no longer detectable due to the decrease in the power per unit area, which falls under the detectability threshold. Similarly, the surface of last contact (SLC) is another sphere that grows from a "D" event and carries the last signal produced by the emitter. The region which is causally connected to the emitter is then limited by these two spheres, and has the shape of a sphere (before the D event) or of a spherical shell (after the D event). The temporal intervals for the communication between two CCNs are represented in the panel (b) of the Figure. The receiver CCN E_1 can listen signals from the emitter CCN E_2 , from the first contact event ($t=C_{12}$) up to the last contact event ($t=B_{12}$). Similarly, the receiver CCN E_2 can listen signals from the emitter CCN E_1 , from $t=C_{21}$ up to $t=B_{21}$.

In this scheme, the entire lifetime of a CCN can then be represented by a polygon, limited in the spatial axis by the maximum distance of the signal D_{max} and in the time axis by the time span between the starting time (A event, concave vertex) and the ending time (D event, convex vertex). This representation allows to easily visualize the important events that result from the existence

and communications of two CCNs (panel (b)). The points in time where the CCNs acquire their communicating capability are dubbed "Awakening" events (A_1 and A_2 in the Figure). Similarly, the points in time where the CCNs lose their communicating capacity are dubbed "Doomsday" events (D_1 and D_2 in the Figure). The points in space-time where the first contact is produced for each one of the CCNs, are defined as "Contact" events, shown as C_1 and C_2 in the Figure. Finally, the two points where the contact is lost for each one of the CCNs, are denominated "Blackout" events, shown as B_1 and B_2 in the Figure. It is important to notice that there is a time delay between the contact events of the two CCNs involved in this analysis, and also a time delay between the two blackout events, so that the time range when a bidirectional contact is possible occurs between the maximum time of the contact points and the minimum time between the blackout points.

A causal connection can be produced without the need of the two involved locations being concurrent or active at the same time. This is a fundamental property of the system which arises as a consequence of the large spatial and temporal scales, where a message is transmitted at light speed. Although a CCN could be active for enough time so as to transmit a message at large distances, the limited power of the message and the dilution that runs as the squared distance from the source, imposes a detectability limit. As a consequence of this limitation and of their finite lifetime, considered

independent variables (hypothesis space)		min. value	max. value	Nbins
τ_a	Mean temporal separation between consecutive awakenings	4000 yr	200 000 yr	50
τ_s	Mean lifetime of a CCN	10000 yr	500 000 yr	50
D_{max}	Maximum reach of a message	(500, 1000, 10000, 20000, 40000, 80000) lyr		6
fixed variables		assumptions		value
	statistical properties of all CCNs	equally distributed		
	Point process for the distribution in time	homogeneous		
f_s	The scan of the sky	fully efficient		1
f_p	panspermia or colonization	absent		0
	shape of the Galactic Habitable Zone	2-dimensional ring		
R_{GHZ}^{min}	Inner radius of the GHZ			20 000 lyr
R_{GHZ}^{max}	Outer radius of the GHZ			60 000 lyr
t_{max}	Time span of the simulation			1.e6 yr
	number of random realizations for each point in the hypothesis space			50
discrete events		affected variables		
A event	Awakening: a CCN starts its communication capabilities	Number of active CCNs		
B event	Blackout: the end of the communication channel stops	Number causal channels		
C event	Contact: a new causal contact is produced	Number of causal channels		
D event	Doomsday: a CCN ends its communication capabilities	Number of active CCNs		

Table 1.: Definition of independent variables and adopted values for fixed parameters that are part of the simulation. Variable parameters define the spatial and temporal structure of the process and the maximum reach of the messages.

as the period of time between the acquisition and loss of communicating capacity, each CCN will fill a spherical shell region of the Galaxy, limited by two concentric spherical surfaces. The leading front, or surface of first contact (SFC) grows from the central CCN until it reaches the maximum distance D_{max} . Thus, the volume reached causally by a CCN is initially a growing sphere.

Following the end of the civilization, there is still a region which is filled with the emitted signals. The trailing front, or surface of last contact (SLC) also grows from the central CCN, with a delay with respect to the SFC equivalent to the lifetime of the CCN, and produces a spherical shell region. Any other CCN within this region will be aware of the originating CCN, even if it has disappeared before the time of contact. This region will grow if the surface of first contact has not yet reached the maximum distance D_{max} , and will shrink otherwise until the surface of last contact reaches D_{max} , producing as a result the loss of all signal from the central CCN. In our approach, we consider a model Galaxy where the width of the disk is negligible with respect to the radius of the disk, so that the CCNs are placed on a 2D plane disk. In the 2D simulation only the intersection of the communicating spherical shells with the plane of the galaxy is relevant, and produce the corresponding circles or rings for the filled spheres or annular regions of the spherical shells, respectively.

The initially growing communicating sphere, is shown over space-time diagrams, where time is represented on the horizontal direction, and space is represented in the vertical direction. In the upper panel (a), the sphere is growing as the surface of first contact has not reached the maximum distance. In the middle panel (b) it has reached the maximum distance, so that it remains at the same size. After a Doomsday event (bottom panel, b), the signals can still be observed, but the surface of last contact grows. We also show in this Figure a schematic representation of two emitters, E_1 and E_2 , that reach each other at different times. The time span for E_i is (A_i, D_i) , for $i = 1, 2$. Emitter i can listen to emitter j between C_{ij} and B_{ij} . The type and length of causal contact in

both directions depend on the distance and time lag between the awakening events, the maximum distance that a signal can reach and the time period in which each emitter is active. In the Fig. 2 we show a schematic representation of the possible cases in which a CCN E can be in causal contact with a CCN R. The duration of the causal contact in one direction depends on several factors, mainly the lifetimes, the time period between the A events and the distance between the two CCNs involved in the causal contact.

The temporal structure of the process is defined by two distribution parameters that represent the mean time interval that an intelligent civilization can emit and receive signals, and the mean time interval between the emergence of an intelligent communicating civilization and the next one. The spatial structure of the simulation is given by the size and shape of the Galactic Habitable Zone and the maximum distance a signal can travel to be detected. The parameters for the temporal distributions also determine the spatial properties since the density of active CCNs in the Galaxy depend on these two parameters. For example, a small τ_a and a large τ_s will produce a Galaxy densely populated with CCNs, and vice versa. Also, some hypotheses must be made in order to complete the simulation. Forgan (2011) argues that the times at which different civilizations become intelligent follow a Gaussian distribution, and then the distribution of inter-arrival times is an inverse exponential. We chose to assume that the distribution of the times of A events is a stationary Poisson process, and then the distribution of the times between the appearance of new consecutive CCNs is exponential. Regarding the duration of a CCN, we propose that the distribution of the duration of CCNs is a stationary exponential distribution. Balbi (2018) stress the fact that it would be desirable to arrive at a theoretical statistical distribution of the lifespan of civilizations, preferentially on the basis of the underlying astrophysical and biological processes. Maccone (2014b) argues that this distribution should be a log normal. (EXPAND)

There is no a temporal window for the model, i.e., the simulation starts when the process is already stable, and ends before

any galactic effect could modify or affect of fixed variables. The probability for the rise of a CCN is homogeneous over the GHZ. Although the Galaxy has a well known spiral structure, the assumed sparsity of civilizations makes this assumption very reasonable. Otherwise, if the distribution of civilizations is not sparse, it could be the case that the spiral arms would host most of the civilizations, and contacts are frequent between closely located civilizations. In such a case we could expect that the interpretation of our results could be considered as pessimist for the establishment of a contact with our planet. We also limit the possibilities of life or other types of civilizations to the hypothesis usually stated for the definition of the GHZ (Dayal et al., 2016; Gonzalez et al., 2001; Lineweaver et al., 2004; Gonzalez, 2005; Morrison & Gowanlock, 2015; Haqq-Misra, 2019; Rahvar, 2017; Gobat & Hong, 2016; Rahvar, 2017). Vukotić & Ćirković (2012) propose probabilistic cellular automata model to explain the astrobiohistorical history of the Milky Way. This means that we set aside possible civilizations that could survive in severe conditions or unstable systems, which would prevent the appearance of life as we know it.

While the aforementioned assumptions are basic conditions for most of the stochastic processes observed in nature, we need to make stronger assumptions related to the nature of the message. The most simple assumption about the message itself, is that it travels at light speed. With this, we are considering messages sent through, for example, electromagnetic radiation or even gravitational radiation, but we set apart messages sent with mechanical means or physical objects, or through some unknown technology that violates the known so far laws of physics. For the communication of CCNs through messages sent isotropically, we assume that the capacity to emit signals and to receive signals occur at the same time. This means that the ability to find another civilization develops at the same time that the ability and intention to emit a signal in all direction, intended to be detected by an unknown civilization. Although there are several reasons to think that this could not be the case, at large time scales it can be considered that both abilities occur roughly at coincident epochs. Another essential assumption is that all CCNs use the same signal power, so that there is a maximum distance out to which it can be detected. It is worth mentioning that we are considering in our experimental setup a system composed by several emitters and receivers across the Galaxy, under the hypothesis proposed before. In such a system we compute probabilities of a CCN making contact with another CCN, and the results must be interpreted as for a randomly chosen CCN, given certain conditions of homogeneity on an ensemble of equivalent galaxies. We stress the fact that we are not centered on the probabilities for the Earth itself, but on a generalized CCN. Regarding the extent of the signals, we know that the distance from which a signal from Earth could be detected using the current technology is of a few hundreds light years, given that the signal was sent to a specific direction.

It is straightforward to propose and implement a distribution of maximum distances, although this would increase the model complexity at the cost of a larger uncertainty or of another dimension on the hypothesis space. This proposal is based on a pronoid scenario (REF), and we do not consider in this work the occurrence of paranoid or partially paranoid civilizations. If that would be the case, the results obtained here can be taken as upper limits.

In our simulations we also assume the simplest situations for the growth of the sphere of first contact. For example, we discard the possibility of stellar colonization (e.g. Newman & Sagan, 1981; Walters et al., 1980; Starling & Forgan, 2014; Barlow, 2013a; Jeong et al., 2000; Maccone, 2011) and assume that the communication aim is performed to all directions with the same power and the same probability, i.e., strongly assume isotropic communication in all cases. More detailed simulations could be produced considering different efficiency of communication or detection methods. However, in this case we also would complicate the experimental setup, make the results less evident. The results are independent of the nature of life (organic or artificial). The lifetime of a civilization can be caused by auto destruction or by external factors.

2.1. Power laws vs. exponential laws

The power law and exponential statistical distributions are among the most common patterns found in natural phenomena. For example, the distribution of the frequency of words in many languages is known to follow a Zipf law (which is a power law). Zipf law also describes population ranks of cities in various countries, corporation sizes, income rankings, ranks of number of people watching the same TV channel (Zipf's law). The magnitudes of earthquakes, hurricanes, volcanic eruptions and floods; the sizes of meteorites or the losses caused by business interruptions from accidents, are also well described by power laws (Sornette 2006). The power law behaviour has been observed in a variety of systems, including for example stock market fluctuations, sizes of computer files and word frequency in languages (Mitzenmacher, 2004; Newman, 2005; Simkin & Roychowdhury, 2006) Power laws have also been widely used in biological sciences, e.g., in analyzing connectivity patterns in metabolic networks (Jeong et al., 2000) and in the number of species observed per unit area in ecology (Martín & Goldenfeld, 2006; Frank, 2009). More examples can be found in the literature (Martín & Goldenfeld, 2006; Maccone, 2010; Barabási, 2009; Maccone, 2014a,b; Benguigui & Marinov, 2016)

In this work, the exponential distribution of lifespan and waiting times is justified by considering the hypothesis that the process of appearance of life in the galaxy is homogeneous and stationary. That is, there is no preferred location within the GHZ for the spontaneous appearance of life, and the emergence of a CCN is independent of the existence of previous CCNs in the galaxy. This is equivalent to proposing a Poisson process for the emergence of CCNs, since there is a close relation between the number of events in time or space and the waiting time or separation, respectively (e.g., Ross, 2012). That is, these are two alternative approaches to describing the same process, a Poisson distribution for the number of events implies an exponential distribution for their separations, and viceversa. It should be emphasized that the exponential laws used in this work are assumed as part of the working hypothesis, and instead of analyzing results from a particular parameter chosen ad-hoc, we explore the hypothesis space and analyze the impact of the values of these parameters on the results.

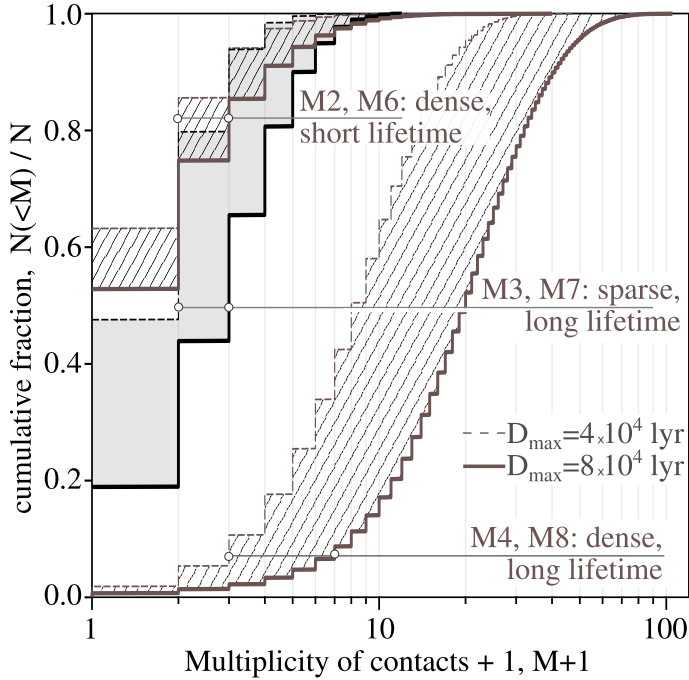


Fig. 3. Empirical cumulative distributions of the number contacts for CCNs in four different samples (M5, M6, M7, M8) with two values for the range of the signal reach: $D_{max}=40000$ ly (blue), and $D_{max}=80000$ ly (orange). Except for the models corresponding to a densely populated galaxy with long-living CCNs, the CCNs which receive more than 10 contacts are very unlikely. See Table 2 for model descriptions.

2.2. Complexity of the model

The odds of a causal contact between two CCNs should not be considered as the odds of a contact between two intelligent civilizations, and in fact the latter could be much lesser than the former. Indeed, in order to establish a contact between any two entities, a minimum degree of compatibility must be accomplished without any previous agreement, making the possibility of a contact with a message that could be deciphered highly rare. There is a trade-off between the simplicity and the complexity of the experiments, and further analysis could be performed following this framework in order to explore possible implications of the results for more detailed configurations. For example, the communication method (isotropic, colimated, serendipitous) can affect the observables, making it necessary to implement a correction factor. Taking this into account, our results regarding the probability of causal contact should be considered as upper limits for effective contacts, since they depend on the efficiency of both the emitter and the receiver to broadcast and scan the sky for intelligent signals, respectively. A correction by coverage ratio in the detection and by a targetting ratio in the emission could be easily implemented in the simulation, although the effect of reducing the probability of contact is basically the product of the efficiency ratios and thus such implementation is not necessary. Therefore, the values of the probabilities could be modified by a constant correction factor equal to the combined emission/reception efficiency (Smith, 2009; Anchordouqui & Weber, 2019; Forgan, 2014). Other considerations include the effects of alignments, the use of stars as

sources or amplifiers, the nature of the message carrier, the use of a spatial distribution that actually resembles the spiral shape and the width of the disc of the Galaxy, different distribution functions for the mean lifetime of CCNs, and different efficiencies for the sphere of the causal region of each CCN resembling different searching strategies (Hippke, 2017). It is also possible to consider that D_{max} is different for different CCNs. For example a power law where powerful emissions are rare and weak emissions are common could be an improvement to the model. In this work we chose not to implement this for the sake of simplicity. Finally, the role of the message contents could influence on the lifespan of a CCN that receives a message, although the implementation of such behaviour would increase the number of free parameters and would be highly speculative.

2.3. Discrete event process

Given a parametric model $M(\tau_a, \tau_s, D_{max})$, which includes the functional forms of the statistical distributions and fixed values for the hypotheses, a discrete event simulation is performed by keeping track of a set of variables that change each time a meaningful event is produced. The main variables that follow the evolution of the simulation are the positions of stars, which are sampled randomly within the GHZ, the time of the awakening of each CCN (A event), and the time of the vanishing of each CCN (D event). The variables that can be deduced from the previous ones include the number of CCNs in casual contact with at least another CCN at a given time, the number of CCNs as a function of time, the number of CCNs that receive a message at least one time, the number of CCNs that receive a message at least one time and successfully deliver an answer and the number distribution of waiting time to receive a message. All these quantities are updated each time one of the four events (A, B, C, D) is produced.

2.4. Model for CCNs

Since the method is based on events, the first step is to define an architecture of events, the relationships between them and how events trigger changes on the state of the system. We consider a simulated system that represents the galactic habitable zone (GHZ). On a first approach, the GHZ is a 2-dimensional annular region. The adopted values for the GHZ are 20 kly and 60 kly, for the inner and outer radius, respectively (Lineweaver et al., 2004). This simple model does not take into account the variations in stellar density given by the spiral structure. Although there are several possible approaches, we chose to follow the evolution of the system according to the following events:

- (A) Awakening: A new CCN acquires the ability to emit and receive messages and starts to actively broadcast and lookout for messages.
- (C) Contact: A new one-way causal contact is established (does not require the awareness of the involved CCNs.)
- (B) Blackout: An existing causal contact is interrupted, with or without the occurrence of a doomsday event.
- (D) Doomsday: An old CCN disappears, or halts its communication activities.

We have chosen this nomenclature so that it can be easily remembered from the initial A, B, C, D. The B event is produced

Model subset	D_{max} [lyr]	τ_a interval [yr]	τ_s interval [yr]	description
M1	40000	[10000, 30000]	[10000, 50000]	dense, short lifetime
M2	40000	[170000, 190000]	[10000, 50000]	sparse, short lifetime
M3	40000	[10000, 30000]	[400000, 440000]	dense, long lifetime
M4	40000	[170000, 190000]	[400000, 440000]	sparse, long lifetime
M5	80000	[10000, 30000]	[10000, 50000]	dense, short lifetime
M6	80000	[170000, 190000]	[10000, 50000]	sparse, short lifetime
M7	80000	[10000, 30000]	[400000, 440000]	dense, long lifetime
M8	80000	[170000, 190000]	[400000, 440000]	sparse, long lifetime

Table 2.: Selected models to analyze the behavior of simulation outputs and their dependence on simulation outputs and their dependence on simulation parameters.

when one of the two CCNs halts in its capability of emitting and receiving signals. It can occur at the same time the D event or before. Similarly, a Contact event can be produced at the time of the Awakening event or later, and there can be several C events for the same CCN.

The system is updated each time an event is produced. The time marks for each event (A and D for each CCN and C and B for each causal contact) are stored as a result of the simulation. Also, the list of active CCNs is obtained as a function of time. Some fixed variables must be set in order to carry out the simulation: the size of the Galactic Habitable Zone, the mean lifetime of a CCN, τ_s , the mean waiting time for the appearance of another CCN, τ_a , and the maximum distance a message can be detected.

The Galactic Habitable Zone is the only one of the four parameters that is barely known, is set at fixed values of the inner and outer radii, radial symmetry is assumed, and the width of the galactic disk is neglected compared to the radial size. The two radii are measured in light years, with the aim to maintain a single and comprehensive unit for both space and time coordinates.

The simulation was implemented on a python 3 code, which is publicly available^a

3. RESULTS: EXPLORING THE PARAMETER SPACE

We implemented the simulation of a regular grid of models varying over the hypothesis space, which covers 15000 different models. For each model, we simulated 50 realizations with different random seeds, in order to perform a MonteCarlo estimation of the variance. The parameters for the temporal aspects of the simulation (the mean waiting time for the next awakening, $\langle\tau_a\rangle$, and the mean lifetime, $\langle\tau_s\rangle$) cover the ranges 4000-200000 yr and 10000-500000 yr, respectively, with a regular partition of 50 values for each parameter. For the D_{max} parameter, we chose the values 500, 1000, 10000, 20000, 40000 and 80000 lyr. This setup makes a total of 750000 simulations, each covering a time range of one million years. In Table 1 we show the three variable parameters, the ranges of their values and the number of bins that have been explored in the numerical experiments. We also show the set of parameters that take part in the simulation, their values and the hypotheses that define the runs of the simulations.

As a product of the simulations, several quantities can be obtained. Some quantities are directly derived from the discrete

events, namely, the ID of emitting and receiving CCNs, the position in the galaxy, and the times of each of the events that are relevant to keep track of the number of CCNs (time of awakening and time of doomsday) and of the number of contacts (the times of contacts and the times of blackouts). We can also derive the additional quantities that represent the properties of the CCNs, for example the total time elapsed between the awakening and the doomsday of each CCN. The time span of a CCN listening another or being listened by another can also be easily derived from the results of a realization. This way we can also compute the distribution in the galaxy of CCNs that reach contact and the waiting time until the first contact or the waiting time until the next contact. Regarding the properties of the population of CCNs and its evolution, the simulation yields the fraction of awaken time a CCN is listening at least another CCN (i.e., in their causal cone), the age of contacted CCNs at first contact, the distribution of time to wait until next contact, the fraction of CCNs where the first contact is given at the awakening, the distribution of the number of contacts for each CCN, the distribution of the number of contacts as a function of CCN age, the number of contacts as a function of time in the galaxy, the rate of CCNs that succeed in contact, and the distribution of distances between contacted CCNs. Another useful derived quantity is the duration of two-way communication channels or the fraction of contacts that admit a response. It is also possible to analyze the relations between the distance to CCN vs. the time of double communication, the distance to CCN vs. the age of contacted CCN, the age of a CCN and the maximum number of contacted CCNs before doomsday, or the lifespan of a CCN vs. the maximum number of contacts. In addition, all these quantities can be analyzed as a function of the simulation parameters. We chose eight models that are on fairly opposed regions of the explored parameter space, and cover short/long lifetimes, short/long waiting times for the next CCN to appear in the Galaxy and short/large range reach of the signal, including all possible combinations. The details of each model are summarized in the Table 2.

In what follows, we focus on the analysis of the duration of contacts (Sec. ??), the waiting time for the first contact (Sec. 3.2.) and the variations of contact possibilities as a function of the position of the CCN in the Galaxy (Sec. 3.3.).

^ahttps://github.com/mlares/simu_contact

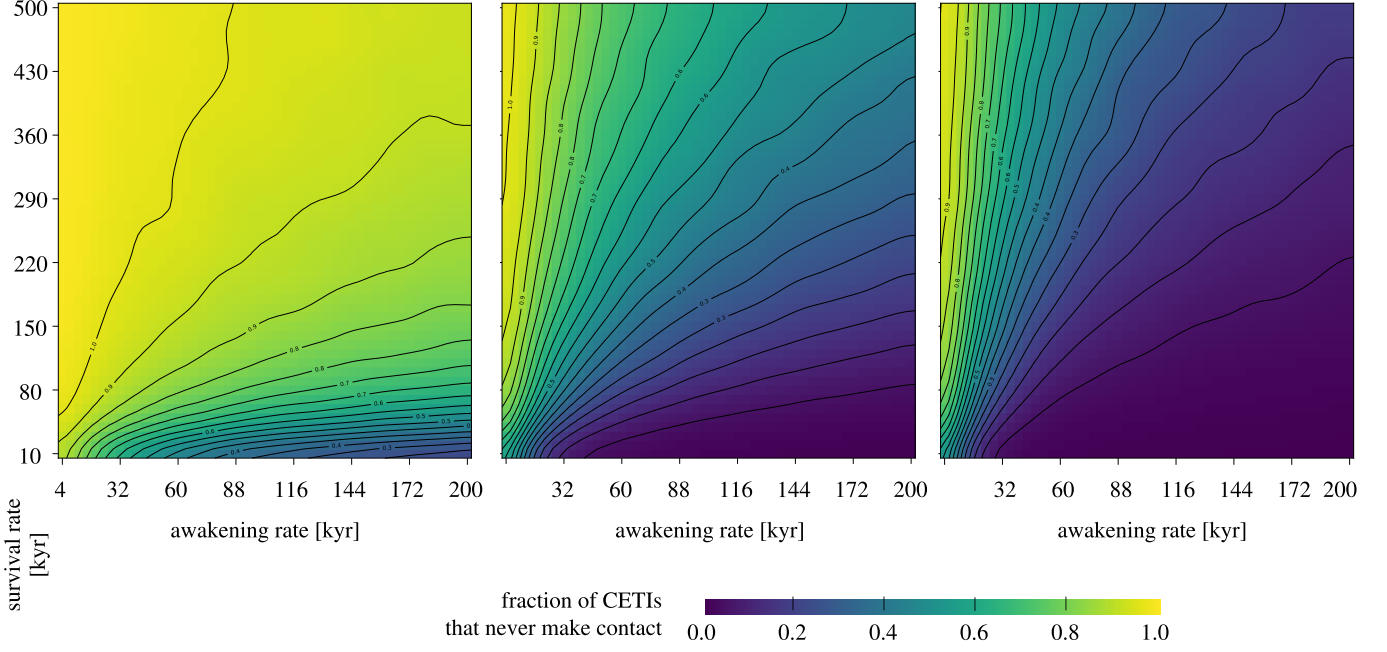


Fig. 4.: Rate of MPLs that never make contact (listening) as a function of τ_a and τ_s , for $D_{max}=10000$ (left panel), $D_{max}=40000$ (middle panel), and $D_{max}=80000$ (right panel)

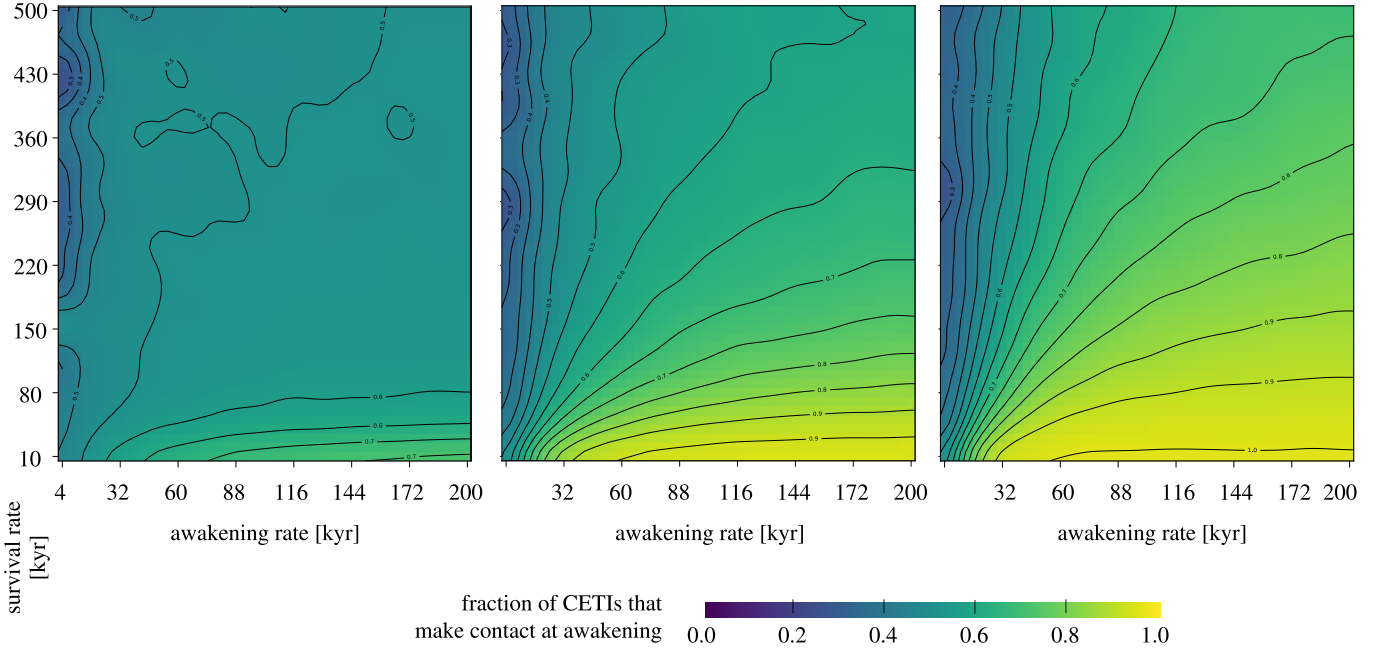


Fig. 5.: Rate of MPLs that listen at the moment of the awakening, as a function of τ_a and τ_s , for $D_{max}=10000$ (left panel), $D_{max}=40000$ (middle panel), and $D_{max}=80000$ (right panel)

3.1. Membership to the network of connected CCNs

In Fig. 3 we show the empirical cumulative distributions of the number contacts for CCNs in six different samples, including short and long lifetimes ($\langle \tau_s \rangle = 10000$ yr and $\langle \tau_s \rangle = 100000$ yr, respectively), dense and sparse spatial distribution ($\langle \tau_a \rangle = 10000$ yr and $\langle \tau_a \rangle = 100000$ yr, respectively),

and two different signal reach ranges ($D_{max}=40000$ lyr and $D_{max}=80000$ lyr). The models M1 and M5 are not shown, since in both cases the total number of contacts is different from zero for less than the five per cent of the CCNs. The areas between models with the same mean lifetime and mean awakening time are shaded for visualization purposes. As it can be seen from this Figure,

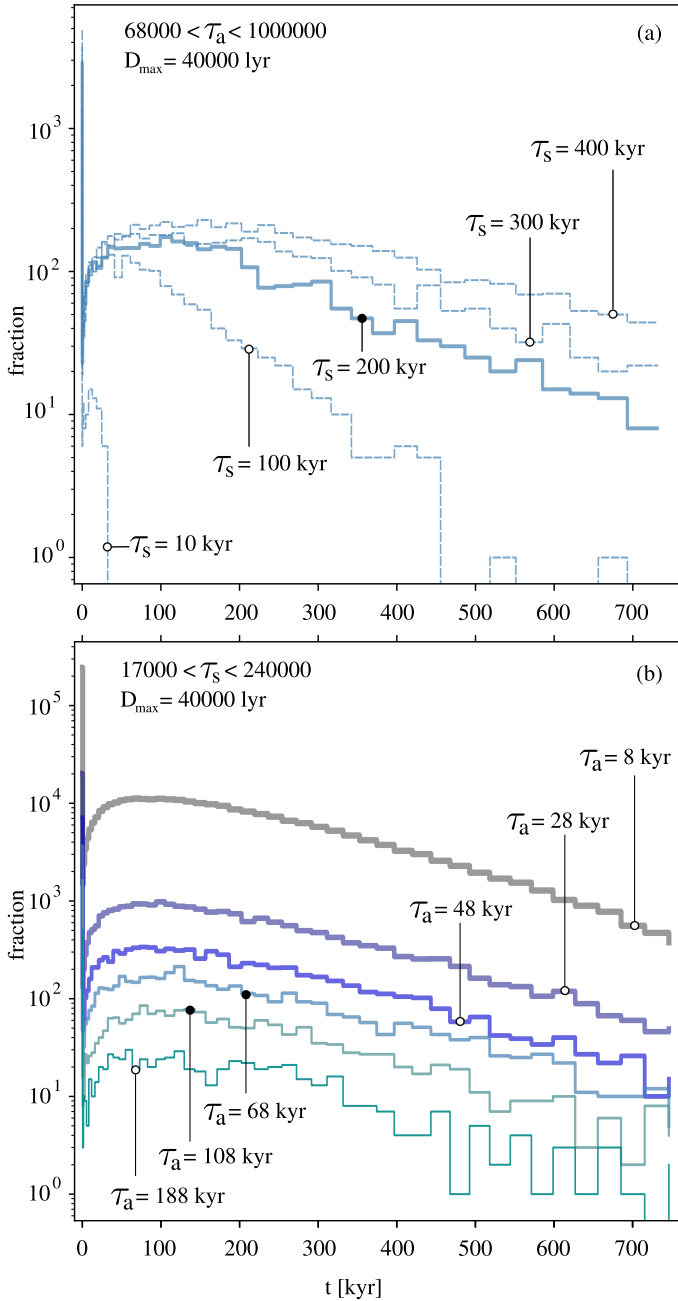


Fig. 6.: Histograms of the mean waiting times for the first contact, for several models. Left panel shows the histograms for several values of τ_a , and τ_s in the range 17000-24000 yr. Right panel shows the histograms for several values of τ_s , and τ_a in the range 68000-100000 yr. The shape of the histograms does not change when τ_a is modified, but significantly changes when τ_s is modified.

the mean lifetime is more determinant than the mean awakening rate (dense and sparse, represented by a different shade) for the number of contacts. As expected, of the samples with the longest D_{max} the model with a dense and sparse in the timeline (low $\langle\tau_a\rangle$) and a long lifetime (high $\langle\tau_s\rangle$), is the model that maximizes the number of contacts, reaching a maximum of order 20 contacts for a single CCN. Similarly, for the models with long

signal range ($D_{max} = 80000 \text{ ly}$), the one which is dense and with long lifetime has the maximum number of contacts, reaching nearly 100 contacts for each CCN in its entire lifetime. This is considerably larger than any model with a shorter lifetime, which produce a number of contacts of at most the order of ten contacts per CCN. A couple of comments are worth to mention about this plot, namely, it has a logarithmic scale on the x-axis, and it is the cumulative, not differential, empirical distribution, so that the differences in the number of contacts for different models is quite large. Another interesting feature observed in this Figure, is that for the models analyzed, there are CCNs that have no causal contacts with any other CCN during their whole lifetime. The fraction of CCNs with no contact ranges from nearly 20% up to nearly 90% (models M1 and M5, not shown), except for the dense and long lifetime models, for which almost all CCNs make at least one contact. Since these results depend on just eight models, we analyze the properties of the frequency of contacts as a function of both the mean lifetime and the mean awakening time. On Fig. 4 we show 2D color maps with the fraction of CCNs in the simulations that never make contact (i.e., never listen to another CCN), as a function of the mean lifetime ($\langle\tau_s\rangle$, in the range 0–500 yr) and the mean awakening time ($\langle\tau_a\rangle$, in the range 0–200 yr), for three different values of the maximum signal range, $D_{max} = 10000 \text{ yr}$ (left panel), $D_{max} = 40000 \text{ yr}$ (middle panel), and $D_{max} = 80000 \text{ yr}$ (right panel). A clear pattern emerges in this Figure, showing that the probability for a CCN of making causal contact with at least another CCN during their entire lifetime, increases with increasing D_{max} , increasing $\langle\tau_s\rangle$ and decreasing $\langle\tau_a\rangle$, following a roughly linear dependence with the three parameters.

While the number of CCNs that do not succeed in reaching the causal contact regions of other node is a useful indicator of degree of isolation, there is also the chance that a number of CCNs are already in the causal contact region of other nodes, which shows a somewhat opposite situation. The fraction of CCNs that make the first contact at the awakening event is shown in the Fig. 5, as a function of the mean lifetime ($\langle\tau_s\rangle$, in the range 0–500 yr) and the mean awakening time ($\langle\tau_a\rangle$, in the range 0–200 yr), for three different values of the maximum signal range, $D_{max} = 10000 \text{ yr}$ (left panel), $D_{max} = 40000 \text{ yr}$ (middle panel), and $D_{max} = 80000 \text{ yr}$ (right panel). These probabilities are consistent with the ones on the previous Figure. Although they are not complementary, it is clear that the dependence with the three parameters is roughly linear in both cases.

3.2. Waiting time for a first contact

In this subsection we analyze the distribution of the waiting times for a first contact. Such distribution can be considered to compute the probability for a random CCN to carry out a SETI project and spend a given time until the first contact is made.

In the Fig. 6 we show the histograms of the mean waiting times for the first contact, for several models. Upper panel (a) panel shows the histograms for several values of the mean survival time τ_s , and the mean awakening time τ_a in the range 68000-100000 yr. Lower panel (b) shows the histograms for several values of τ_a , and τ_s in the range 17000-24000 yr. As it can be seen, the shape of the histograms is almost the same when τ_a is modified (panel (b)), but significantly changes when τ_s is modified (panel (a)). For

different values of τ_a , the shape of the distribution is similar, and the main difference is given by the different number of contacts on the different models. Conversely, for different values of τ_a , the shape of the distribution is similar, and the main difference given by the different number of contacts on the different models.

The fraction of the CCNs that have made at least one contact as a function of the elapsed time since the awakening, is computed with respect to the total number of nodes that make causal contact at least one time in the time range from the Awakening up to the Doomsday events. From a frequentist approach, the total counts from the awakening ($t = 0$ yr) up to a given time are related to the estimation of the probability of listening during that time interval and reaching to causal contact region of at least another node. The complement of this value is the probability of observing in a time interval with no success, i.e., without ever happening a Contact event. Clearly, this probability diminishes with time and tends to zero for large time periods. The differential probability of making a causal contact reach its maximum at the awakening event for all models. That is, for a short period of time like the nearly 50 years SETI programs have been active, the initial moment is the most promising for making a (causal) contact, at least for a given technology. This consideration offers a new approach for SETI programs, where the search for new communication technologies has a fundamental role.

3.3. Location within the Galaxy

For this model, the majority of CCNs do not make any contact during all the time period in which they are active. As expected, the fractions of CCNs making at least one contact diminishes as the number of contacts rises. The shape of this distribution is a result of the geometry of the GHZ. In general, a closer position to the center of the Galaxy slightly favours the possibility of a contact. This would indicate that the position of the Earth is suitable for the odds of making a contact.

4. DISCUSSION

We have implemented a suite of simulations following a stochastic approach, to explore the hypothesis space of a simple model that accounts for the causal connections between communicating civilizations on a simplified galaxy. The different models can be generated with a minimal number of free parameters and some fixed assumptions. We argue that three parameters can be used to describe a variety of situations, ranging from a Galaxy where an intelligent civilization is very rare, to a Galaxy populated with plenty of civilizations in causal contact. With this approach, we can estimate several quantities as a function of the parameters on the hypothesis space, so we explored the outcomes of different models that arise as by-products of the simulations.

For instance, it is possible to estimate the timescale for an uninterrupted SETI effort to reach success, in terms of different model parameters that reflect different, so far unknown, scenarios for the appearance of intelligent life on the galaxy.

Although the simulations use a number of speculative assumptions, we argue that the degree of knowledge about the origin and persistence of life in the Galaxy does not worth the implementation of more detailed or sophisticated models. Instead, we

take advantage of the simplicity of the model to explore the hypothesis space, i.e., the three-dimensional parameter space of the parametric model, in order to gain insight on the consequences of different scenarios for the search of intelligent life. Our analysis is not centered in obtaining the odds for the Earth to make contact with another intelligent civilization. Instead, we focus on obtaining a statistical, parameter dependent description of the possible properties of the communication networks that comprise sets of nodes with broadcasting and reception capabilities. This causally connected nodes are sparsely distributed in both space and time, making it difficult the analytical treatment and justifying the simulation approach.

Under the hypotheses of our experiments, we conclude that a causal contact is extremely unlikely unless the Galaxy is heavily populated by intelligent civilizations. Roughly, in order to have at least one contact in the entire lifetime of the CCN, there should appear at least one CCN every ~ 20000 yr, with a mean active period of at least ~ 30000 yr. There is a balance between the density of CCNs and the mean lifetime since, as expected, a lower density can be compensated by a longer active time period. In all cases, for a short period of time (for instance, the time SETI programs have been active on Earth), the maximum probability of making a contact occurs at the moment of the awakening. This suggests the possibility that an alternative SETI strategy could be the search for alternative message carriers, for the case in which the search has not been performed on the adequate channels.

Acknowledgement. This work was partially supported by the Consejo Nacional de Investigaciones Científicas y Técnicas (CONICET, Argentina), the Secretaría de Ciencia y Tecnología, Universidad Nacional de Córdoba, Argentina, and the Universidad Católica de Córdoba, Argentina. This research has made use of NASA's Astrophysics Data System. Plots and simulations were made with software developed by the authors using R and python languages. Plots were postprocessed with inkscape.

Disclosure statement. No competing financial interests exist.

References

- Anchordoqui L. A., Weber S. M., 2019, arXiv e-prints
- Balb A., 2018, *Mem. della Soc. Astron. Ital.*, 89, 425
- Balbi A., 2018, *Astrobiology*, 18, 54
- Barabási A. L., 2009, *Science* (80-.), 325, 412
- Barlow M. T., 2013a, *Int. J. Astrobiol.*, 12, 63
- Barlow M. T., 2013b, *Int. J. Astrobiol.*, 12, 63
- Benguigui L., Marinov M., 2016, A classification of the natural and social distributions Part 2: the explanations. Tech. rep.
- Bloetscher F., 2019, *Acta Astronaut.*, 155, 118
- Chung C. A., 2003, *Simulation Modeling Handbook: A Practical Approach* (Industrial and Manufacturing Engineering Series). CRC press
- Ćirković M. M., 2004, *Astrobiology*, 4, 225
- Conway Morris S., 2018, *Int. J. Astrobiol.*, 17, 287
- Dayal P., Ward M., Cockell C., 2016, arXiv e-prints
- Drake F., 1962
- Enriquez J. E. et al., 2017, *Astrophys. J.*, 849, 104
- Fogg M. J., 1987, *Icarus*, 69, 370

- Forgan D., Dayal P., Cockell C., Libeskind N., 2016, *Int. J. Astrobiol.*, 16, 60
- Forgan D. H., 2009, *Int. J. Astrobiol.*, 8, 121
- Forgan D. H., 2011, *Int. J. Astrobiol.*, 10, 341
- Forgan D. H., 2013, *JBIS - J. Br. Interplanet. Soc.*, 66, 144
- Forgan D. H., 2014, *JBIS - J. Br. Interplanet. Soc.*, 67, 232
- Forgan D. H., 2017a, *Int. J. Astrobiol.*, 16, 349
- Forgan D. H., 2017b, *Int. J. Astrobiol.*, 16, 349
- Forgan D. H., 2019, *Int. J. Astrobiol.*, 18, 189
- Forgan D. H., Rice K., 2010, *Int. J. Astrobiol.*, 9, 73
- Frank S. A., 2009, *The common patterns of nature*
- Funes J. G., Florio L., Lares M., Asla M., 2019, *Theol. Sci.*, 0, 1
- Glade N., Ballet P., Bastien O., 2012, *Int. J. Astrobiol.*, 11, 103
- Gobat R., Hong S. E., 2016, *Astron. Astrophys.*, 592
- Gonzalez G., 2005, *Orig. Life Evol. Biosph.*, 35, 555
- Gonzalez G., Brownlee D., Ward P., 2001, *Icarus*, 152, 185
- Haqq-Misra J., 2019, arXiv e-prints
- Haqq-Misra J., Kopparapu R. K., 2018, *Habitability of the Universe Before Earth*, 307
- Harp G. R. et al., 2018, *Astrophys. J.*, 869, 66
- Hinkel N., Hartnett H., Lisse C., Young P., 2019, *Bull. Am. Astron. Soc.*, 51, 497
- Hippke M., 2017, arXiv e-prints
- Horvat M., 2006, *Int. J. Astrobiol.*, 5, 143
- Horvat M., Nakić A., Otočan I., 2011, *Int. J. Astrobiol.*, 11, 51
- Jeong H., Tombor B., Albert R., Oltvai Z. N., Barabasi A. L., 2000, *Nature*, 407, 651
- Lampton M., 2013, *Int. J. Astrobiol.*, 12, 312
- Lineweaver C. H., Fenner Y., Gibson B. K., 2004, *Science (80-.)*, 303, 59
- Lingam M., Loeb A., 2018, *Astrobiology*, 19, 28
- Loeb A., Batista R. A., Sloan D., 2016, *J. Cosmol. Astropart. Phys.*, 2016, 040
- Loeb A., Zaldarriaga M., 2007, *J. Cosmol. Astropart. Phys.*, 1
- Maccone C., 2010, *Acta Astronaut.*, 67, 1427
- Maccone C., 2011, *Orig. Life Evol. Biosph.*, 41, 609
- MacCone C., 2011, *Acta Astronaut.*, 68, 63
- MacCone C., 2013, *Int. J. Astrobiol.*, 12, 218
- Maccone C., 2014a, *Int. J. Astrobiol.*, 13, 290
- Maccone C., 2014b, *Acta Astronaut.*, 105, 538
- Maccone C., 2015, *Acta Astronaut.*, 115, 277
- Martín H. G., Goldenfeld N., 2006, *Proc. Natl. Acad. Sci. U. S. A.*, 103, 10310
- Mitzenmacher M., 2004, *Internet Math.*, 1, 226
- Morrison I. S., Gowanlock M. G., 2015, *Astrobiology*, 15, 683
- Murante G., Monaco P., Borgani S., Tornatore L., Dolag K., Goz D., 2015, *Mon. Not. R. Astron. Soc.*, 447, 178
- Newman M., 2005, *Contemp. Phys.*, 46, 323
- Newman W. I., Sagan C., 1981, *Icarus*, 46, 293
- Peters T., 2018, *Int. J. Astrobiol.*, 17, 282
- Prantzos N., 2013, *Int. J. Astrobiol.*, 12, 246
- Ptolemaeus C., 2014, *System Design, Modeling, and Simulation. Using Ptolemy II. Ptolemy.org, Berkeley*, p. 690
- Rahvar S., 2017, *Mon. Not. R. Astron. Soc.*, 470, 3095
- Ross S. M., 2012, *Simulation. Elsevier Science Publishing Co Inc*
- Simkin M. V., Roychowdhury V. P., 2006, *J. Math. Sociol.*, 30, 33
- Smith R. D., 2009, *Int. J. Astrobiol.*, 8, 101
- Solomonides E., Kaltenegger L., Terzian Y., 2016, 228th AAS, San Diego, 228, 1
- Sotos J. G., 2019, *Biotechnology and the lifetime of technical civilizations*
- Starling J., Forgan D. H., 2014, *Int. J. Astrobiol.*, 13, 45
- Tarter J., 2001, *Annu. Rev. Astron. Astrophys.*, 39, 511
- Tarter J. et al., 2009, *Astro2010 Astron. Astrophys. Decad. Surv. Sci. White Pap. no. 294*, 2010
- Vakoch D. A., Dowd M. F., 2015, *The drake equation: Estimating the prevalence of extraterrestrial life through the ages*, Vakoch D. A., Dowd M. F., eds. Cambridge University Press, Cambridge, pp. 1–319
- VanHouten M. A., 2018, *Lancet Gastroenterol. Hepatol.*, 3, 382
- Vukotić B., Čirković M. M., 2012, *Orig. Life Evol. Biosph.*, 42, 347
- Vukotić B., Steinhauser D., Martinez-Aviles G., Čirković M. M., Micic M., Schindler S., 2016, *Mon. Not. R. Astron. Soc.*, 459, 3512
- Walters C., Hoover R. A., Kotra R., 1980, *Icarus*, 41, 193
- Wright J. T., Cartier K. M. S., Zhao M., Jontof-Hutter D., Ford E. B., 2015, *Astrophys. J.*, 816, 17